Algorithm for reconstruction images obtained by a holographic camera based on the Fast Fourier Transform

Nikolay Yudin [1,2,3*], *Mikhail* Zinovev[1,2], *Vladimir* Kuznetsov[1], *Maxim* Kulesh[1,3], *Sergey* Podzyvalov[1], *Elena* Slyunko[1], *Henry* Heimbuch[3], and *Hussein* Baalbaki[1]

[1]National Research Tomsk State University, 634050, Lenin Ave. 36, Tomsk, Russia
[2]Institute of Optics and Atmosphere SB RAS V.E. Zuev, Academician Zuev sq. 1, Tomsk, Russia
[3]IGS LLC, 634040, Vladimir Vysotsky St., 28, building 7, Tomsk, Russia

Abstract. In this work, a prototype of a holographic camera was developed that allows for the determination of the location and linear dimensions of volumetric defects in semiconductor materials. For the efficient operation of the holographic camera, in addition to optimizing the optical scheme, an algorithm was developed to accelerate the process of reconstructing digital holograms, since the significant amount of holographic data obtained requires a significant increase in the performance of processing holographic images. The developed algorithm bases on a fast Fourier transform with a mixed radix, which allows increasing the reconstructing time of digital holographic images by more than two times compared to standard algorithms.

1 Introduction

Digital holography is employed for the identification and measurement of particles of various natures in diverse media [1-5]. A holographic camera setup has been designed for recording digital holographic images of volumetric optical and semiconductor materials containing bulk defects; subsequent layer-by-layer numerical reconstruction of images of cross-sections of the investigated volume with a specified step; fixation of longitudinal coordinates of each cross-section; detection of sections containing focused images of defects (longitudinal focusing, similar to microscopy); and determination of longitudinal and transverse coordinates, sizes, shapes of particles, and their recognition.

A digital hologram is a discrete two-dimensional array of digitized intensity values of the interference pattern of the reference and object waves [1]. This array is taken as the distribution (up to a constant) of the field in the plane of the hologram. This distribution is used as the initial one, and the numerical calculation [2] of the diffraction integral allows calculating the field distribution (and then the intensity) in the plane at a given distance from the plane of the hologram, i.e., in the corresponding cross-section of the studied volume. At

* Corresponding author: rach3@yandex.ru

the same time, it becomes possible to identify the plane of the defect location in three-dimensional space.

To address this task, a holographic camera setup was developed. For efficient operation of the holographic camera, in addition to optimizing the optical scheme of the device, optimal selection of the laser source and matrix receiver, there is a need for algorithms capable of significantly accelerating the process of digital hologram reconstruction. This is due to the large volume of holographic data obtained, which requires a significant increase in the performance of holographic image processing.

Discrete Fourier Transform (DFT) and Inverse Discrete Fourier Transform (IDFT) algorithms are used for digital hologram reconstruction. The number of operations required in DFT has a complex power dependence on the dimension of the calculated data array (in our case, digitized intensity values in the hologram recording plane). For reconstruction of a digital hologram recorded by a high-resolution CCD matrix, a significant number of operations is required. In practice, various Fast Fourier Transform (FFT) algorithms are often used. These algorithms require significantly fewer computational operations for transformation compared to DFT and allow increasing the calculation speed by more than 2 times. Existing low-order FFT algorithms cannot be applied to large data arrays, and mixed-radix FFT is only applicable to data arrays of specific sizes.

Therefore, the goal of the work was to develop both the holographic camera setup itself and a modified FFT algorithm that allows processing large holographic data arrays (with a bit depth of 1500 or more) of arbitrary size, obtained from this setup. The algorithm was tested on digital hologram data arrays obtained using the developed holographic camera.

2 Optical scheme of the holographic camerasetup

A holographic camera setup, as shown in Figure 1, was developed as part of this project.

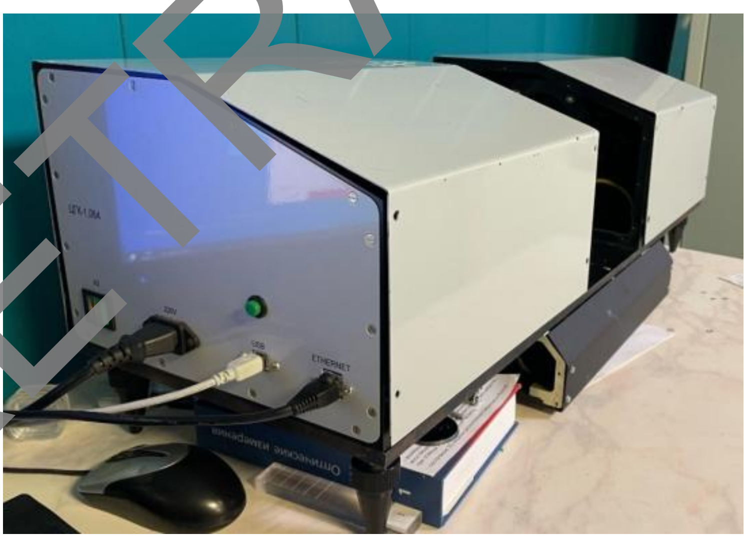

Fig.1. The developed setup of the holographic camera.

The developed setup allows recording the interference pattern of the reference and object waves using a CCD or CMOS matrix. Figure 2 shows the axial scheme of Gabor holography used in the creation of the holographic camera setup.

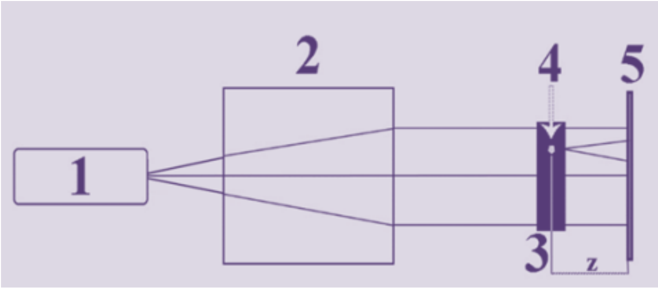

Fig.2. Diagram of the holographic camera setup. 1 – Radiation source with a wavelength of 1.064 μm, 2 – beam expander, 3 – test sample (ZGP crystal), 4 – defect in the crystal volume, 5 – recording device - CCD matrix.

A laser diode with a wavelength of 1.064 μm is used as a source of the reference wave. The light beam from the emitter is expanded using a beam expander (collimator) (2). According to the optical scheme, the radiation falls on the sample (3), part of which is diffracted by bulk defects (4) inside the sample being studied, forming so-called object waves. The interference pattern of the reference wave, which passed through the sample without diffraction, and the object wave (diffracted by the defective structure of the sample) is recorded digitally using a CCD matrix. Thus, a digital hologram is recorded.

The developed holographic camera setup, in general, consists of three main units as shown in Figure 3, including the radiation source unit (1), the cuvette compartment unit for installing the sample under study (2), and the radiation receiver unit (3).

Fig. 3. Main units of the developed holographic camera setup.

The source unit (1) includes a pair of laser diodes with wavelengths of 1.064 μm and 650 nm, the radiation of which is combined using a fiber optic combiner. The laser diode with a wavelength of 650 nm is auxiliary, operating in the visible range (red color), and is necessary for visual positioning of the sample in the cuvette compartment. Also, this unit contains electronic components for powering the electronics, as well as for data transmission.

The cuvette compartment unit (2) is a compartment with a motorized table that can move in three directions. The sample is placed on the table, and the desired location on the sample is selected using the red laser beam. The three-coordinate movement for more precise positioning of the studied area of the sample is available using a computer.

The receiver unit (3) is a compartment containing a digital camera with a CCD or CMOS matrix. The source unit (1) and the receiver unit (3) are connected by a system of power cables, as well as low-current cables for data transmission. The matrix used in the work had an image resolution of up to 2048x2048 pixels, with a matrix pixel size of 3.5 µm. The main characteristics of the developed holographic camera are presented in Table1.

Table 1. The main characteristics of the developed holographic camera setup.

Characteristic	Value
Wavelengths	1.064 µm + 0,650 µm
Radiant power	Up to50 mW
Field of view	100 × 80 mm
Matrix resolution	2048 × 2048 (pixel size3.5 µm)
Tested material thickness	45 cmand more (depending on the absorption coefficient of the material)
Frame rate for dynamic recording	Up to 120 frames in second

3 Algorithm for reconstructing images obtained from a holographic camera

A digital hologram is a discrete two-dimensional array of digitized intensity values of the interference pattern of the reference and object waves [1]. This array is taken as the distribution (up to a constant) of the field in the plane of the hologram (U(x1,y1)). This distribution is used as the initial one, and the numerical calculation [1] of the diffraction integral (1) allows calculating the distribution of the field (and then the intensity) in the plane at a given distance from the plane of the hologram U(x2,y2) (that is, in the corresponding cross-section of the studied volume).

$$U(x_2,y_2)=\frac{1}{i\lambda z}\int_{-\infty}^{\infty}\int_{-\infty}^{\infty}U(x_1,y_1)e^{i\frac{2\pi}{\lambda}z}e^{\frac{i\pi}{z\lambda}((x_1-x_2)^2+(y_1-y_2)^2)}dx_1dy_1 \qquad (1)$$

whereλ is the wavelength, z is the distance between the hologram plane and the reconstruction plane.

Accordingly, layer by layer, an image of the studied volume of the sample can be formed. In this case, in each reconstructed image of the cross-section of the single crystal, defects (inhomogeneities) are visualized, and it becomes possible to determine their size, shape, orientation, and location in the single crystal.

To solve this integral, the Fourier transform is used. As is well known, the Fourier transform is an operation that maps one function of a real variable to another function, a complex variable. This new function describes the coefficients in the expansion of the original function into elementary components - harmonic oscillations with different frequencies. The Fourier transform in analytical form is presented in formula (2).

$$\hat{f}(\omega)=\frac{1}{\sqrt{2\pi}}\int_{-\infty}^{+\infty}f(x)e^{-ix\omega}\,dx \qquad (2)$$

The Discrete Fourier Transform (DFT) can be conditionally divided into the following components: Let x_0, x_1,..., x_{n-1} be a sequence of complex numbers; The analytic function is presented as a polynomial: f(x) = $t_0+t_{1x}+t_{2x2}+\ldots+t_{n-1x2}$; which can be represented as an array.

The Discrete Fourier Transform is performed according to formula 3.

$$\omega_k = \sum_{n=0}^{N-1} x_n \times e^{\frac{2\pi i}{N}kn} \quad (k = 0,\ldots,N-1), \tag{3}$$

The result of the DFT will be a polynomial array. Let's consider n points on the complex plane: ω_0, ω_1, ...,ω_{n-1}; Next, we perform the inverse Fourier transform according to formula (4).

$$\omega_k = \sum_{n=0}^{N-1} x_n \times e^{\frac{-2\pi i}{N}kn} \quad (k = 0,\ldots,N-1), \tag{4}$$

This set of numbers is called the Discrete Fourier Transform of the initial set, where N is the number of signal values, x_n are the measured signal values, and k is the frequency index. This transformation is reversible; for the numbers f^0,..., f_{n-1}, there exists a unique polynomial f(t) of degree no higher than n-1 with such values z_0, ..., z_{n-1} respectively. The formula for the inverse Fourier transform is:

$$\{x_n\} = \sum_{k=0}^{N-1} z_k \times e^{\frac{-2\pi i}{N}kn} \quad (n = 0,\ldots,N-1), \tag{5}$$

where N is the number of signal values, z_k are the complex amplitudes of the sinusoidal signals, k is the frequency index, $\{x_n\}$ are the measured signal values, and i is the imaginary unit.

The number of addition operations (X) for calculating the DFT from N sample points:

$$X = (N-1) * N \tag{6}$$

The number of multiplication operations (Y) for calculating the DFT for an N-dimensional array of numbers:

$$Y = N^2 \tag{7}$$

Total number of operations (Z):

$$Z = X + Y = (N-1) * N + N^2 \tag{8}$$

Let's consider the mixed-radix FFT algorithm. This Fourier transform can be performed in 3 steps. For example, let's consider a polynomial of 15 values (Figure 4).

№1	№2	№3	№4	№5	№6	№7	№8	№9	№10	№11	№12	№13	№14	№15

Fig. 4 . Polynomial, indicating the ordinal numbers of the values.

The polynomial will be reshaped into a matrix structure consisting of five columns and three rows. In such a way that the values are written into a row with a step of three (Figure 5).

№1	№4	№7	№10	№13
№2	№5	№8	№11	№14
№3	№6	№9	№12	№15

Fig. 5. Matrix representation of a polynomial.

The next step will be to calculate the DFT for the numbers in each row of the matrix (Figure6).

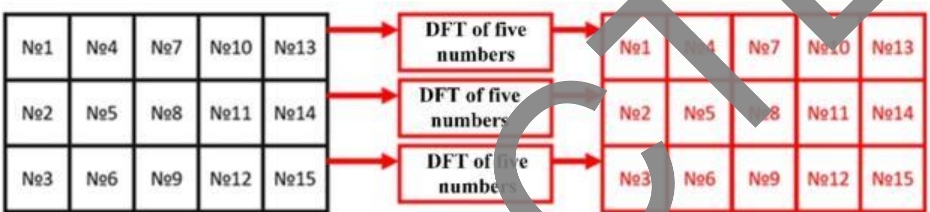

Fig. 6. DFT calculation for the numbers of each row of the matrix.

Let's introduce a twiddle factor:

$$WN_{m*\frac{h}{N}} = e^{\frac{i*\pi*M*H}{N}}, \tag{9}$$

where m is the row number of the element, h is the column number of the element (counting starts from zero, not one); i is the imaginary unit; N is the number of elements.
Multiply each element by its corresponding multiplier (Figure 7).

	0	1	2	3	4
0	№1	№4	№7	№10	№13
1	№2	№5*WN1/15	№8*WN2/15	№11*WN3/15	№14*WN4/15
2	№3	№6*WN2/15	№9*WN4/15	№12*WN6/15	№15*WN8/15

Fig.7. Multiplication of each matrix element by its corresponding turning coefficient.

As can be seen from Figure 7, some multipliers are repeated. This is due to the identical ratio of multiplying the row number of an element by the column number, divided by the total number of elements.
After multiplying all elements by the twiddle factor, the final step is the DFT for each column of elements (Figure 8).

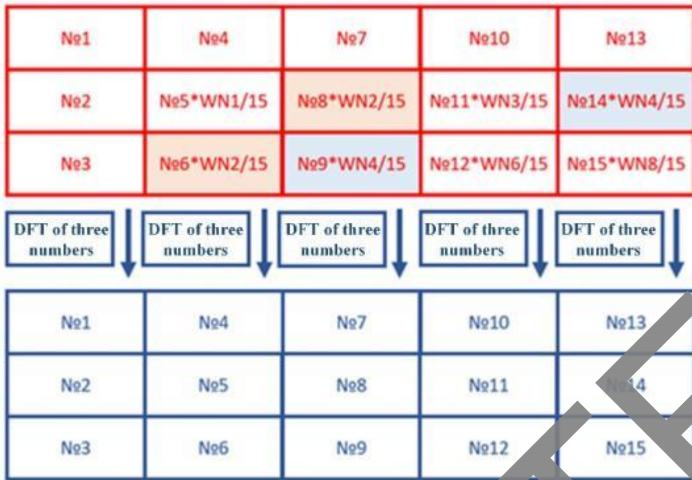

Fig.8. DFT calculation for the numbers of each column of the matrix.

After the inverse transformation of the matrix into an array, the transformed polynomial is obtained using the mixed-radix FFT method (Figure 9).

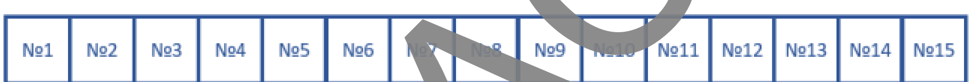

Fig. 9. Converted polynomial using the FFT method using a mixed base.

Let's consider the case of a mixed-radix FFT where an array is with 15 numbers. Instead of a direct DFT an FFT of order 5 will be performed (Figure 10).

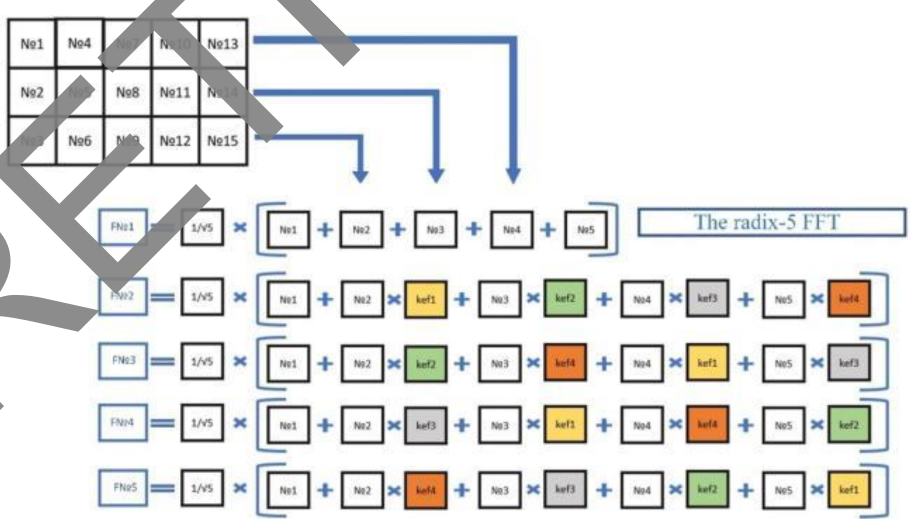

Fig.10. Mixed radix FFT for an array of 15 numbers.

https://doi.org/10.1051/bioconf/202413802032

Next, for each column, the twiddle factors will be calculated in turn. These will be added as a multiplier for the coefficients of the radix-3 FFT. In this way, a radix-3 FFT will be performed, and supplemented by a twiddle factor for each column (Figure 11).

Let's introduce the twiddle factor

$$WN_{m*h/N} = e^{\frac{i*\pi*M*H}{N}}, \tag{10}$$

where m is the row number of the element, h is the column number of the element (indexing starts from zero, not one); i is the imaginary unit; M is the number of rows; H is the number of columns; N is the number of elements.

Then

$$X(m,h) = \sum_{h} X(m,h) * WN_{m*h/N} \tag{11}$$

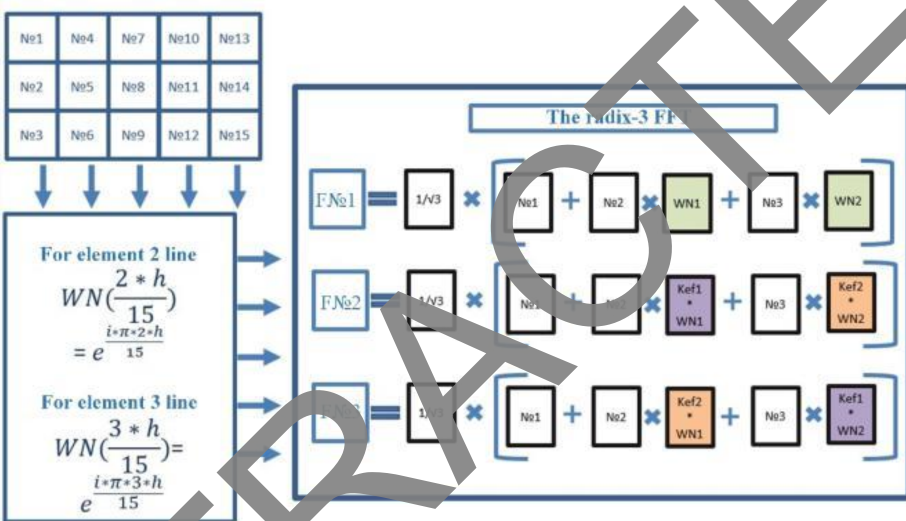

Fig.11. The radix-3 FFT supplemented with twiddle factor for each column.

As is clearly seen from Figure 11, regardless of the numerical values (№1-№15) of the input array, the values of the multiplication coefficients will not change. The values of the coefficients are influenced by the total number of values in the array and the order of the transform

$$X_{(k*h)} = e^{\frac{i*\pi*k*h}{N}} * kef(h), \tag{12}$$

where $X_{(k*h)}$ is the multiplication factor, k and h are the column and row indices respectively, N is the total number of elements in the array, $kef^{(h)}$ is the fast Fourier transform coefficient for small orders, and depends only on the row index.

To avoid repeatedly calculating the multiplication coefficient for each pixel, the once-calculated coefficients were saved to a file, from which they were then extracted as needed during algorithm execution (Figure 12). A separate file was created for each array size. Moving the coefficients to a separate file reduced the number of mathematical operations by an average of 65%. Consequently, the algorithm execution speed increased accordingly.

As can be seen from formula 12, since iπ is a constant, the value of X(kh) depends on the ratio (kh/N) and the row number (since the fast Fourier transform coefficient of small orders depends on it). Consequently, some coefficients may be repeated. To avoid coefficient duplication, the data storage structure in the file consists of a key (kh/N), row number, and the value itself. This allows for a reduction in the amount of data stored in the file and decreases its size.

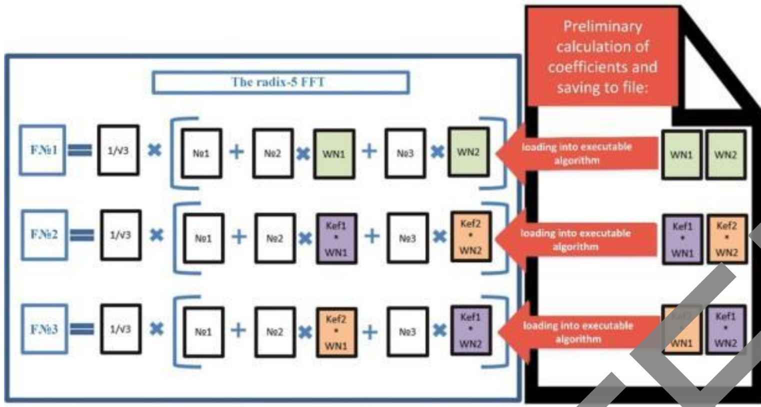

Fig. 12. Diagram of using a template file to increase the speed of the executing algorithm.

If the number of samples is very large, there will be no change in the algorithm, except for the addition of more divisions (Figure 13).Dividing the array into subarrays will occur until the final value of the array length is equal to a small order, or is significantly reduced

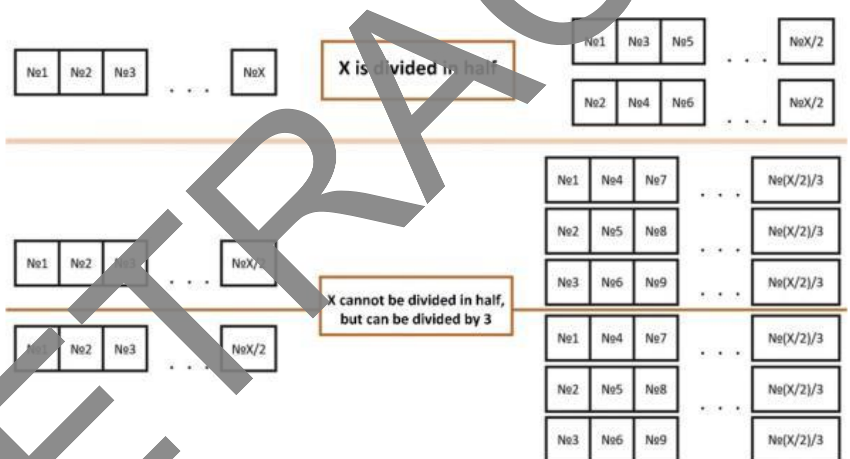

Fig. 13. The process of dividing the array.

4 Program Algorithm

Function for User Input:

- Input 2D array of intensity values for the object wave I(x,y) and reference wave B(x,y). The program extracts the number of samples N from this array.
- Wavelength of the light source λ;
- Physical size of the matrix pixel;
- Gamma correction degree γ;
- Analyzed distance interval of the radiation passing from the CCD matrix Δd;
- Discretization step d;

- Number of threads loading the CPU processor.

Function for Loading an Image from a CCD Matrix and Obtaining a Pixel Array.Since a black-and-white image encoded in RGBa (R-red, G-green, B-blue, a-alpha) is used, the function adds only the red component of each pixel to the array. The other 3 values (green, blue, and alpha) are discarded.

Function for Loading an Executable Module with Hologram DecryptionCode. The executable code is launched simultaneously on multiple cores. The number of cores is specified in the input data function.

Calculation of the Convolution Kernel (formula 13) for each pixel and writing the values to an array.

$$\omega = \frac{1}{\mathrm{i}d\lambda} e^{\frac{\mathrm{i}\pi}{\lambda d}\left(\left(x-\frac{N}{2}\right)^2+\left(y-\frac{N}{2}\right)^2\right)} \qquad (13)$$

The FFT for pixel values of the input image and convolution kernel values are parallel calculated in a single function. Since the FFT algorithm requires a significant number of sorting operations, to save resources, the calculation of the required transforms is performed in parallel. This allows for a 30% speedup in the calculation. Before the calculation begins, it is necessary to convert the values of the convolution kernel and the values of the image pixels into a matrix form; for this, a separate function is used. The FFT calculation is first performed in parallel for each row of values of the matrices, the number of which depends on the horizontal resolution of the hologram. Then, the FFT is performed for each column of values of the matrices, the resolution of which depends on the vertical resolution of the hologram. Next, the inverse recording from two matrices are converted into two data arrays.

Sequential multiplication of the i-th element of the array of transformed image values with the i-th element of the transformed convolution kernel values is applied (see formula 14). The result is written into a single array.

$$u = F([I(x,y)B(x,y)]) \times F\left(\frac{1}{\mathrm{i}d\lambda} e^{\frac{\mathrm{i}\pi}{\lambda d}\left(\left(x-\frac{N}{2}\right)^2+\left(y-\frac{N}{2}\right)^2\right)}\right) \qquad (14)$$

The inverse DFT (IDFT) is calculated for the obtained array, then it is written to a new array, and the maximum value is determined as following

$$U = F^{-1}(u) \qquad (15)$$

Testing of a Digital Holographic Image Reconstruction Program

To test the reconstruction programof digital holographic image, an optically transparent object containing a model particle in the shape of a perfect square on its back side is placed in a holographic camera (Figure 14). It is known that this particle is located at a distance of 80-82 mm from the CCD matrix. Next, a hologram is recorded, and it is loaded into the developed program, with the recording parameters entered beforehand (Figure 15).

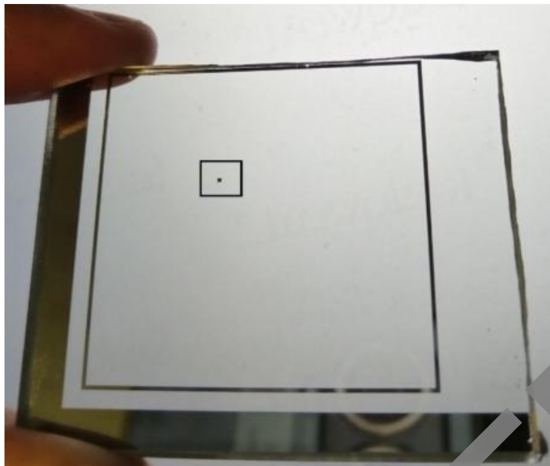

Fig. 14. Test object.

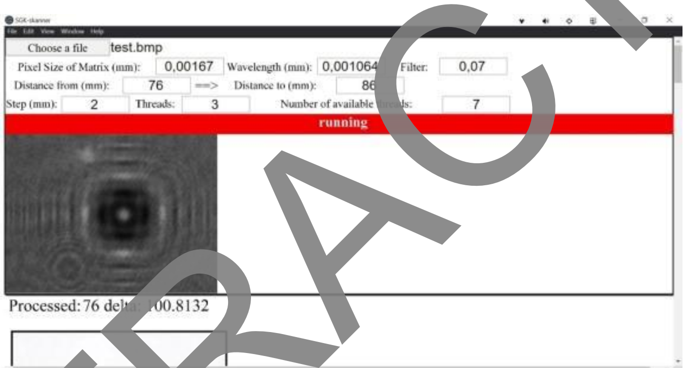

Fig.15. Screenshot of the program.

Next, the program proceeds with hologram reconstruction on the specified planes. From the reconstruction results (Figure 16), it is clear that the plane of best focus is located at 80-82 mm on the reconstructed images. This coincides with the actual location of the defect.

Fig. 16. Reconstructed holographic images.

5 Conclusion

The work describes the development of a holographic camera setup and a corresponding image reconstruction algorithm for analyzing defects within a sample. The algorithm employs the Discrete Fourier Transform (DFT) and a mixed-radix FFT approach for reconstructing images from the captured holograms. Pre-calculated coefficients are stored in files and reused during processing, which allows to reduce the number of mathematical operations by an average of 65%. The system was tested with a sample containing a model particle. The reconstructed image successfully identified the particle's location, demonstrating the effectiveness of the developed setup and algorithm.

Overall, this project demonstrates a promising approach for using holographic imaging to analyze defects within samples. The combination of the custom camera setup and the efficient reconstruction algorithm allows for detailed and accurate analysis.

6 Acknowledgements

The results were obtained as part of the implementation of the state assignment of the Ministry of Education and Science of Russia, project No. FSWM-2020-0038.

References

1. R. Collier, C. Burkhart, L Lin. Optical Holography (1971)
2. V.V. Dyomin, A.I. Gribenyukov, A.S. Davydova, M.M. Zinovev, A.S. Olshukov, S.N. Podzyvalov, I.G. Polovtsev, N.N Yudin, Applied Optics, **58**, 34 (2019) DOI: 10.1364/AO.58.00G300
3. Reinhard W. Meier, Optical society of america, 55, 8 (1965) doi:10.1364/JOSA.55.000987
4. W. Huaying, Z. Baoqun, W. Yi, Z. Li, W. Guangjun, W. Dayong, Proc. SPIE 6622, *"Depths of view and focus of digital holographic imaging system"*, International Symposium on Photoelectronic Detection and Imaging 2007: Laser, Ultraviolet, and Terahertz Technology, 662213 (2008) doi.org/10.1117/12.790818
5. V. V. Dyomin, A. Yu. Davydova, I. G. Polovtsev, N. N. Yudin, M. M. Zinovev, Digital Holography, Atmospheric and oceanic optics, **36**, 2 (2023) DOI:10.1134/S1024856023030041